

## Biosynthesis of (MWCNTs)-COOH/CdO hybrid as an effective catalyst in the synthesis of pyrimidine-thione derivatives by water lily flower extract

Shahrbano Kaveh , Navabeh Nami , Banafsheh Norouzi & Ali Mirabi

To cite this article: Shahrbano Kaveh , Navabeh Nami , Banafsheh Norouzi & Ali Mirabi (2020): Biosynthesis of (MWCNTs)-COOH/CdO hybrid as an effective catalyst in the synthesis of pyrimidine-thione derivatives by water lily flower extract, Inorganic and Nano-Metal Chemistry, DOI: [10.1080/24701556.2020.1841229](https://doi.org/10.1080/24701556.2020.1841229)

To link to this article: <https://doi.org/10.1080/24701556.2020.1841229>



Published online: 12 Nov 2020.



Submit your article to this journal [↗](#)



Article views: 11



View related articles [↗](#)



View Crossmark data [↗](#)



# Biosynthesis of (MWCNTs)-COOH/CdO hybrid as an effective catalyst in the synthesis of pyrimidine-thione derivatives by water lily flower extract

Shahrbano Kaveh, Navabeh Nami, Banafsheh Norouzi, and Ali Mirabi

Department of Chemistry, Qaemshahr Branch, Islamic Azad University, Qaemshahr, Iran

## ABSTRACT

Pink Water lily flower, with the scientific name of *Nymphaea alba* in the family of Nymphaeaceae, was collected from North of Iran, Mazandaran in spring, dried in shade and powdered. The powdered flower material was extracted in 70% (vol/vol) ethanol. Acid functionalized multi-walled carbon nanotubes/CdO (MWCNTs-COOH/CdO) was fabricated by using the Water lily flower extract. The presence of CdO nanoparticles and their surface conjugation to MWCNT have been confirmed by FT-IR, X-ray diffraction, transmission electron microscopy, scanning electron microscopy and energy-dispersive X-ray spectroscopy. It was used as a highly efficient catalyst for the synthesis of some pyrazolo[3,4-*d*]pyrimidine and pyrido[2,3-*d*]pyrimidine derivatives. These compounds were synthesized by the reaction of some substituted pyrazole or pyridine, thiourea and I<sub>2</sub> in the presence of MWCNTs-COOH/CdO hybrid (5% mol) in warm water. The assigned structure was further established by CHN analyses, NMR and FT-IR spectra.

## ARTICLE HISTORY

Received 25 April 2020  
Accepted 18 October 2020

## KEYWORDS

Water lily flower extract; biosynthesis; MWCNTs-COOH/CdO; nonocomposite; pyrimidine-thione derivatives

## Introduction

Multi-walled carbon nanotubes (MWCNTs) were the first kind of carbon nanotubes (CNTs) to be reported and they have attracted much attention due to their unique physical and chemical properties and also many potential applications such as drug delivery,<sup>[1,2]</sup> electronics,<sup>[3]</sup> catalysis,<sup>[4-6]</sup> biosensors,<sup>[7]</sup> biomedical,<sup>[8]</sup> storage,<sup>[9]</sup> and photovoltaic<sup>[10]</sup> activities.

It has been indicated that the MWCNTs properties can be dramatically influenced by surface modification with chemical and biological compounds.<sup>[11,12]</sup> Nanometal and nanometal oxide particles immobilized MWCNTs have shown excellent catalytic properties in organic reactions.<sup>[13]</sup> Many metal oxides and sulfides have been used to modify the MWCNTs.<sup>[14,15]</sup> Due to the presence of a high surface area of MWCNT-COOH/MxOy hybrid, it can be employed as an alternative catalyst supports, high dispersion, outstanding stability, and convenient catalyst recycling.<sup>[16]</sup> On the other hand, CNTs are effective supports for nanometal particles (NPs) like zinc oxide, cadmium oxide (CdO), nickel oxide or manganese oxide, and together they represent hybrid structures (NP-CNTs) that combine the unique properties of both.<sup>[17]</sup> CdO is one of the most attractive semiconductor materials. It has a tunable bandgap, which proves to be a useful catalyst,<sup>[18]</sup> sensor,<sup>[19]</sup> nonlinear material,<sup>[20]</sup> solar cell<sup>[21]</sup> and antibacterial device.<sup>[22]</sup>

The scientists are very interested in the biosynthesis of nanomaterials using plants because this method focuses on the production of the desired product without producing harmful intermediate byproducts during the chemical

reaction.<sup>[23,24]</sup> *Nymphaea alba* belongs to the Nymphaeaceae family to know as Water lily or Lotus is an aquatic flowering plant.<sup>[25]</sup> This plant grows in the wetland and slightly acidic water. The roots and stems of water lily are in the water; the broad leaves are on the surface of water toward the sun and flowers are in the air. *Nymphaea alba* contains some active chemical compounds like alkaloids, gallic acid, sterols, flavonoids, glycosides, tannins, and polyphenolic compounds,<sup>[26,27]</sup> because of them all parts of the plant especially the flower extract have been used in photochemistry.<sup>[28]</sup>

According to the above reasons, we predict that the combination of CdO nanoparticles and acid functionalized multi-walled CNTs can be helpful to increase catalytic activity for the synthesis of heterocyclic compounds. So in this paper, we present a simple and inexpensive biosynthesis of MWCNTs-COOH/CdO hybrid using pink Water lily flower extract in good yield and under mild reaction conditions. MWCNT-COOH/CdO hybrid was used as an effective catalyst for the synthesis of some pyrazolo[3,4-*d*]pyrimidine and pyrido[2,3-*d*]pyrimidine derivatives by reaction of some substituted pyrazole or pyridine with thiourea and I<sub>2</sub> in warm water.

## Experimental

### Chemicals and instrumentation

All chemicals and solvents were purchased from Merck and Aldrich. The production of nano compounds were monitored by measuring the UV-Vis spectrophotometer

(JENWAY 650), in the wavelength range of A200 to A800 nm and determined by powder X-ray diffraction (XRD) PW 3040/60 X'Pert PRO diffractometer system, using Cu K $\alpha$  radiation with ( $\lambda=1.5418 \text{ \AA}$ ) in the range of  $2\theta=20\text{--}80^\circ$  at room temperature. The morphology and sizes of NPs were evaluated using a scanning electron microscope (SEM) and transmission electron microscope (TEM, 150 kV, and Philips-CM 10) by Day Petronic Company-Iran. FT-IR measurements were recorded on a Shimadzu 8400s spectrometer with KBr plates. The NMR spectra were recorded on Bruker XL 400 (400 MHz) instruments; Mass-spectrometric measurements were made on an Agilent 6890 N Network GC system. The C, H, N analyses were performed by the microanalytical service of Daypetronic Company. Melting points were determined on an Electrothermal 9100 without further corrections.

### Collection and preparation of purple water lily flower extract

Purple Water lily flower, with the scientific name of *N. alba*, was collected from the wetland in the north of Iran, Mazandaran. The flower was first washed thoroughly in DI water, dried at room temperature for one week and then ground in a blender before extraction.

The powdered Water lily flower was weight (500 g) in a beaker and percolated with 70% (vol/vol) ethanol. This beaker was properly covered with aluminum foil and left for 72 h. The solution was then filtered using a funnel filled in a filter paper and the extract obtained. It was concentrated using a rotary evaporator and stored in the refrigerator at 4 °C prior to use.

### Synthesis and purification of MWCNTs-COOH

a) MWCNT (250 mg) was mixed with 200 mL concentrated nitric acid and the mixture was refluxed for 8 h followed by its ultracentrifugation at 10,000 rpm. The functionalized MWCNTs were dispersed in 500 mL distilled water followed by filtration through a cellulose nitrate membrane filter (0.45  $\mu\text{m}$  pore size) using a vacuum filtration assembly. The sample was repeatedly washed with distilled water till neutral pH of the filtrate. The filtered compound was dried in a vacuum oven at 80 °C for 24 h and obtained MWCNTs-COOH were characterized using different techniques.<sup>[29]</sup>b) Water Lily flower extract (1 g) and MWCNTs (0.5 g) were dissolved in 50 ml of ethanol: H<sub>2</sub>O with a ratio of 1:1. The mixture was kept in ultrasonicator for 30 min and then stirred for 2 h at room temperature. The mixture was stirred for 48 extra hours. The precipitate was washed and then centrifuged 3–4 times with distilled water, dried at 100 °C for 2 h and calcined at 350 °C for 3 h.

### Preparation of MWCNTs-COOH/CdO hybrid

Water Lily Flower extract (0.5 g) and the functionalize MWCNTs-COOH (0.3 g) were dispersed into 50 ml of ethanol: H<sub>2</sub>O (1:1) by ultrasonication for 30 min. Under constant

magnetic stirring, the aqueous solution of Cd(NO<sub>3</sub>)<sub>2</sub> (0.02 M, 50 mL) was added dropwise into the reaction mixture through a dropping funnel and gently stirred at 60 °C using temperature-controlled magnetic stirrer for 2 h, after that 0.02 M NaOH was added dropwise to the solution to achieve the pH 10. The mixture was stirred for 24 extra hours. The completion of the reaction was monitored by UV-Vis spectra at 300–600 nm ( $\lambda_{\text{maxes}}=221,274,401 \text{ nm}$ ). After completion of the reaction, the precipitate was purified by several re-dispersions in deionized water and then centrifuged at 8000 rpm for 20 min, dried at 100 °C. The solid samples were then calcined at 350 °C for 3 h.

### General procedure for the synthesis of 4-amino-8H-pyrido[2,3-d]pyrimidine-2-thione and 1,7-dihydro-pyrazolo[3,4-d]pyrimidine-6-thione derivatives using MWCNTs-COOH/CdO

2-Oxo-1,2-dihydro-pyridine-3-carbonitrile derivatives (1 mmol), thiourea (1 mmol) and a catalytic amount of MWCNTs-COOH/CdO (5 mol %) were mixed in warm distilled water (10 ml), I<sub>2</sub> (1.2 mmol) was added in small portions to the solution and stirred. The progress of the reaction was monitored by TLC using *n*-hexane: ethyl acetate (1:1) and detected by a UV lamp (254 and 366 nm). At the end of the reaction, the catalyst was separated by centrifugation, filtered, washed with ethanol and water, dried at 100 °C for 1 h and reused for the same reaction. A small amount of tar was filtered from the residue of the reaction mixture; to the clear filtrate was added sodium hydroxide (2 M) until the solution was just neutered to litmus and the products precipitate. The light yellow or white precipitate was filtered, washed with water and recrystallized from ethanol. The products were determined by CHN analyses, NMR and FT-IR spectra.

### Characterization methods

#### 4-Amino-7-isopropyl-1H-pyrido(2,3-d)pyrimidine-2-thione 1

Reaction of thiourea with 6-isopropyl-2-oxo-1,2-dihydro-pyridine-3-carbonitrile and I<sub>2</sub>.

FT-IR (KBr, cm<sup>-1</sup>): 3100–3500 (NH, NH<sub>2</sub>), 3000 (CH<sub>Ar</sub>), 2921 (CH<sub>Aliph</sub>), 1653 (C=N, C=C), 1447 (C=S). <sup>1</sup>H-NMR (DMSO, 400 MHz,  $\delta$  ppm): 8.03 (d, 1H,  $J=8.8 \text{ Hz}$ , CH<sub>Ar</sub>), 6.61 (s, 1H, NH), 6.25 (dd, 1H,  $J=8.8, 4.0 \text{ Hz}$ , CH<sub>Ar</sub>), 5.47 (br, 2H, NH<sub>2</sub>), 2.82 (m, 1H, CH), 1.17 (m, 6H, 2CH<sub>3</sub>). <sup>13</sup>C-NMR (DMSO, 75 MHz,  $\delta$  ppm): 189.29, 160.15, 149.63, 141.64, 117.26, 102.20, 75.58, 32.39, 21.45. Anal. Calc. for C<sub>10</sub>H<sub>12</sub>N<sub>4</sub>S (220.29): C, 54.52; H, 5.49; N, 25.43, found: C, 54.82; H, 5.58; N, 25.31.

#### 4-Amino-6,7-dimethyl-1H-pyrido(2,3-d)pyrimidine-2-thione 2

Reaction of thiourea with 5,6-dimethyl-2-oxo-1,2-dihydro-pyridine-3-carbonitrile and I<sub>2</sub>

FT-IR (KBr, cm<sup>-1</sup>): 3446 (NH, NH<sub>2</sub>), 3015 (CH<sub>Ar</sub>), 2922 (CH<sub>Aliph</sub>), 1662 (C=N), 1627 (C=C), 1444 (C=S). <sup>1</sup>H-

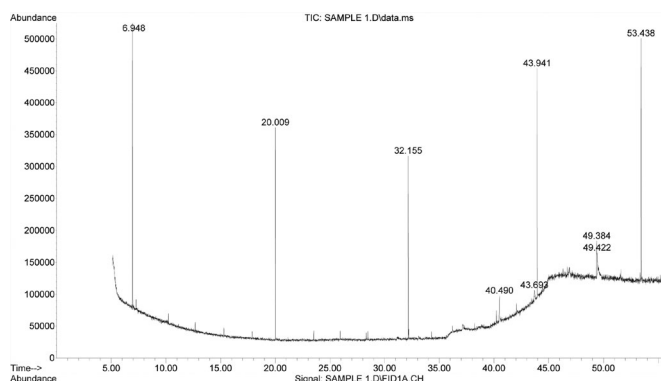


Figure 1. GC-MS Chromatogram of pink Water Lily flower extract.

NMR (DMSO, 400 MHz,  $\delta$  ppm): 7.94 (s, 1H, CH<sub>Ar</sub>), 6.64 (s, 1H, NH), 5.42 (br, 2H, NH<sub>2</sub>), 2.23 (s, 3H, CH<sub>3</sub>), 1.98 (s, 3H, CH<sub>3</sub>). <sup>13</sup>C-NMR (DMSO, 75 MHz,  $\delta$  ppm): 184.58, 160.15, 149.63, 141.64, 117.26, 102.20, 75.58, 32.39, 21.45. Anal. Calc. for C<sub>9</sub>H<sub>10</sub>N<sub>4</sub>S (206.27): C, 52.41; H, 4.89; N, 27.16, found: C, 52.56; H, 4.92; N, 27.21.

#### 4-Amino-5,7-dimethyl-1H-pyrido(2,3-d)pyrimidine-2-thione 3

Reaction of thiourea with 4,6-dimethyl-2-oxo-1,2-dihydro-pyridine-3-carbonitrile and I<sub>2</sub>

FT-IR (KBr, cm<sup>-1</sup>): 3446 (NH, NH<sub>2</sub>), 3032 (CH<sub>Ar</sub>), 2922 (CH<sub>Aliph</sub>), 1653 (C=N, C=C), 1447 (C=S). <sup>1</sup>H-NMR (DMSO, 400 MHz,  $\delta$  ppm): 6.98 (s, 1H, CH<sub>Ar</sub>), 6.60 (s, 1H, NH), 5.48 (br, 2H, NH<sub>2</sub>), 2.25 (s, 3H, CH<sub>3</sub>), 2.19 (s, 3H, CH<sub>3</sub>). <sup>13</sup>C-NMR (DMSO, 75 MHz,  $\delta$  ppm): 174.41, 160.32, 158.62, 143.48, 138.54, 113.53, 108.60, 32.45, 25.95. (GC-Mass): *m/z* Calculated: 206; Observed: 207 (*M* + 1). Anal. Calc. for C<sub>9</sub>H<sub>10</sub>N<sub>4</sub>S (206.27): C, 52.41; H, 4.89; N, 27.16, found: C, 52.46; H, 4.88; N, 27.25.

#### 4-Amino-7-methyl-1H-pyrido[2,3-d]pyrimidine-2-thione 4

Reaction of thiourea with 6-methyl-2-oxo-1,2-dihydro-pyridine-3-carbonitrile and I<sub>2</sub>.

<sup>1</sup>H-NMR (DMSO, 400 MHz,  $\delta$  ppm): 8.00 (d, 1H, *J* = 7.2 Hz, CH<sub>Ar</sub>), 6.93 (s, 1H, NH), 6.21 (d, 1H, *J* = 7.2 Hz, CH<sub>Ar</sub>), 5.44 (br, 2H, NH<sub>2</sub>), 2.26 (s, 3H, CH<sub>3</sub>). <sup>13</sup>C-NMR (DMSO, 75 MHz,  $\delta$  ppm): 186.26, 161.30, 158.16, 154.36, 149.45, 117.26, 105.89, 99.72, 19.64. Anal. Calc. for C<sub>8</sub>H<sub>8</sub>N<sub>4</sub>S (192.24): C, 49.98; H, 4.19; N, 29.14, found: C, 49.92; H, 4.23; N, 29.36.

#### 4-Amino-7-phenyl-1H-pyrido[2,3-d]pyrimidine-2-thione 5

Reaction of thiourea with 2-oxo-6-phenyl-1,2-dihydro-pyridine-3-carbonitrile and I<sub>2</sub>

Yellow powder. FT-IR (KBr, cm<sup>-1</sup>): 3473 (br, NH, NH<sub>2</sub>), 3000–3020 (CH<sub>Ar</sub>), 1629 (C=S), 1442 (C=C). <sup>1</sup>H-NMR (DMSO, 400 MHz,  $\delta$  ppm): 8.02 (d, 1H, *J* = 7.6 Hz, CH<sub>Ar</sub>), 7.49–7.98 (m, 5H, CH<sub>Ar</sub>), 7.21 (d, 1H, *J* = 7.6 Hz, CH<sub>Ar</sub>), 6.98 (s, 1H, NH), 5.64 (br, 2H, NH<sub>2</sub>). <sup>13</sup>C-NMR (DMSO, 75 MHz,  $\delta$  ppm): 182.31, 167.03, 163.20, 160.36, 139.54, 137.14, 129.73, 128.34, 1119.13, 107.28, 102.34. Anal. Calc.

for C<sub>13</sub>H<sub>10</sub>N<sub>4</sub>S (254.31): C, 61.40; H, 3.96; N, 22.03, S, 12.61, found: C, 61.85; H, 3.90; N, 21.94; S, 12.50.

#### 1-Phenyl-6-thioxo-1,5,6,7-tetrahydro-pyrazolo[3,4-d]pyrimidin-4-one 6

Reaction of thiourea with 5-amino-1-phenyl-1H-pyrazole-4-carboxylic acid ethyl ester and I<sub>2</sub>

FT-IR (KBr, cm<sup>-1</sup>): 3454 (br, NH, NH<sub>2</sub>), 3013 (CH<sub>Ar</sub>), 1658 (N-CO-), 1627 (C=N, C=C), 1444 (C=S). <sup>1</sup>H-NMR (DMSO, 400 MHz,  $\delta$  ppm): 7.54–7.56 (m, 2H, CH<sub>Ar</sub>), 7.43–7.49 (m, 3H, CH<sub>Ar</sub>), 7.30 (s, 1H, CH<sub>pyrazole</sub>). Anal. Calc. for C<sub>11</sub>H<sub>8</sub>N<sub>4</sub>OS (244.27): C, 54.09; H, 3.30; N, 22.94, S, 13.3, found: C, 54.72; H, 3.51; N, 22.38; S, 13.56.

#### 4-Amino-3-methyl-1-phenyl-1,7-dihydro-pyrazolo[3,4-d]pyrimidine-6-thione 7

Reaction of thiourea with 5-amino-3-methyl-1-phenyl-1H-pyrazole-4-carbonitrile and I<sub>2</sub>

FT-IR (KBr, cm<sup>-1</sup>): 3443 (br, NH, NH<sub>2</sub>), 3010 (CH<sub>Ar</sub>), 2993 (CH<sub>aliph</sub>), 1653 (NH-CO-O), 1630 (C=N, C=C), 1452 (C=S). <sup>1</sup>H-NMR (DMSO, 400 MHz,  $\delta$  ppm): 7.38–7.536 (m, 5H, CH<sub>Ar</sub>), 6.63 (br, 2H, NH<sub>2</sub>), 2.16 (s, 3H, CH<sub>3</sub>). Anal. Calc. for C<sub>12</sub>H<sub>11</sub>N<sub>5</sub>S (257.31): C, 56.01; H, 4.31; N, 27.22; S, 12.46, found: C, 56.22; H, 4.33; N, 27.34; S, 12.50.

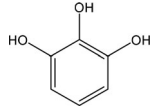
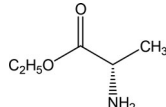
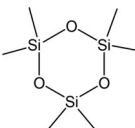
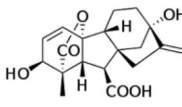
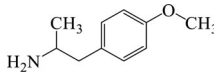
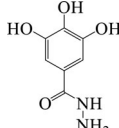
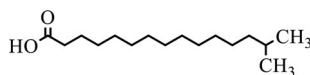
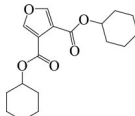
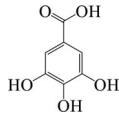
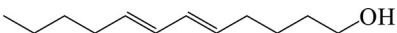
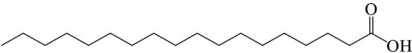
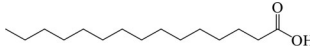
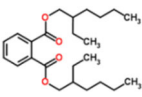
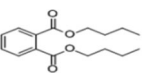
## Results and discussion

The present paper reports the results of a research aimed to verify biosynthesis of the MWCNT-COOH/CdO hybrid from pink Water Lily flower extract as an effective catalyst on heterocyclic reactions. GC-Mass analyze (Figure 1) of the Water Lily flower was performed and various bioactive compounds were identified (Table 1).

#### Optimization of different parameters

The effects of the reaction conditions such as the ratio of plant extract and Cd(NO<sub>3</sub>)<sub>2</sub>, MWCNTs-COOH, pH, reaction time and reaction temperature were studied to maximize the yield of the nano compounds. The resulting solutions of the reaction were monitored using a UV-Vis spectrophotometer. The influence of pH on the synthesis of CdO/MWCNT-COOH was investigated to 3.0, 5.0, 7.0, 8.0, 9.0, 10 and 11 (pH of Water Lily flower extract solution was about 3.0). The reaction completion time was studied by monitoring the absorption spectra of nano compounds formed in the reaction media at different duration's time (10 min to 48 h). Different ratios of plant extract and cadmium nitrate solution were investigated (1:1, 1:2, 1:3, and 1:4) in order to find the maximum production of nano powders. The temperature of the reaction was set at 25 °C, 45 °C, 65 °C and 85 °C using the Water bath for optimization of the reaction temperature. The optimized condition of the reaction was obtained at room temperature in pH = 10 after 24 h with the ratio 1:1 of plant extract and cadmium nitrate solution.

**Table 1.** Phytocomponents of pink Water Lily flower extract by GC-MS.

Molecular formula (MF)	Name of the compound	Structure
$C_6H_6O_3$	1,2,3-Benzenetriol	
$C_5H_{11}NO_2$	L-Alanine ethyl ester	
$C_6H_{18}O_3Si_3$	Cyclotrisiloxane, hexamethyl-	
$C_{19}H_{22}O_6$	Gibberellin A3	
$C_{10}H_{15}NO$	p-methoxyamphetamine	
$C_7H_8N_2O_4$	3,4,5-Trihydroxybenzhydrazid	
$C_{16}H_{32}O_2$	Pentadecanoic acid, 14-methyl	
$C_{18}H_{24}O_5$	Dicyclohexyl furan-3,4-Dicarboxylate	
$C_6H_5AsF_2$	Arsine, diethylphenyl	
$C_7H_6O_5$	Benzoic acid, 3,4,5-trihydroxy	
$C_{10}H_{16}$	Cyclooctene, 3-ethenyle	
$C_{12}H_{22}O$	(5E,7E)-Dodecadien-1-ol	
$C_{18}H_{36}O_2$	Octadecanoic acid	
$C_{15}H_{30}O_2$	Pentadecanoic acid	
$C_{24}H_{38}O_4$	Bis(2-ethylhexyl) phthalate	
$C_{16}H_{22}O_4$	1,2-Benzenedicarboxylic acid	
$C_{20}H_{42}$	Eicosane	

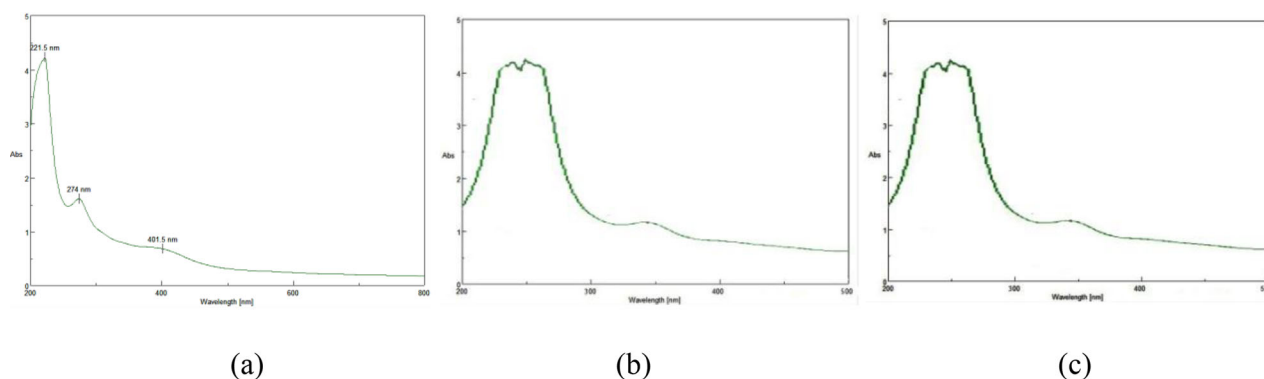


**Figure 2.** UV-Vis spectrum of biosynthesized MWCNT-COOH/CdO after 24 h with the ratio of  $\text{Cd}(\text{NO}_3)_2$ : water Lily flower extract (a) 1:1, (b) 1:2, (c) 1:3.

### UV-Vis studies

Completion of the reaction between Water lily flower extract, MWCNT-COOH, and cadmium nitrate was monitored and optimized by taking the absorption spectrum in UV-Vis spectrophotometer at different reaction conditions. As the Water lily flower extract was added to aqueous cadmium nitrate solution, the color of the solution changed to colloidal dark brown with MWCNT-COOH/CdO colloids formation. The UV-Vis spectra recorded after 10 min, 20 min, 60 min, 16 h and 24 h at different temperatures ( $25^\circ\text{C}$ ,  $45^\circ\text{C}$ ,  $60^\circ\text{C}$  and  $90^\circ\text{C}$ ) from the initiation of reaction at the wavelength of 200–800 nm. Absorption UV-Vis spectra of biosynthesized MWCNTs-COOH/CdO hybrid showed  $\lambda$  maxes at 221, 274 and 401 nm (Figure 2). These results were in line with the findings of other studies.<sup>[30,31]</sup> It is well known from absorption spectroscopy that the band gap increases on decreasing particle size. There is also an opposite ratio between band gap and the wavelength of absorption. The absorption bands of the synthesized MWCNT-COOH/CdO nanocomposite have been shows a blue shift. This optical phenomenon indicates that these nanoparticles show the quantum size effect and can be due to a high decrease in particle size.<sup>[32,33]</sup>

The UV-Vis spectra showed that MWCNT-COOH/CdO was obtained rapidly within the first 30 min only and the MWCNT-COOH/CdO in solution remained stable even after 24 h of completion of reaction at room temperature.

### Thermal properties of (MWCNTs)-COOH/CdO nanocomposite (TGA/DTA)

Differential thermal analysis (DTA) and thermal gravimetric analysis (TGA) of (MWCNTs)-COOH/CdO nanocomposite were carried out. From the thermal decomposition (TGA/DTA) results, several observations are worth to mention. It was performed in order to estimate the final amount, and consequently the thermal behavior of nanocomposite. Eventual MWCNTs oxidation is expected to form  $\text{CO}_2$  gas, leaving the sample and resulting in composite weight loss as a function of temperature. It was investigated in the 25–1000  $^\circ\text{C}$  temperature range. typical thermal TGA and DTA curves are given in Figure 3. There is no weight loss in the range 0–350  $^\circ\text{C}$ , which indicates the absence of coordinated or uncoordinated water molecules. The exothermic

DTA peaks at 356 and 486  $^\circ\text{C}$  were recorded. After about 480  $^\circ\text{C}$ , the samples start to present a significant mass loss, being. This is attributed to the decomposition of MWCNTs into  $\text{CO}_2$  by the  $\text{O}_2$  atmosphere. The oxidation peak, observed in DTA curves, occurs at about 529  $^\circ\text{C}$ . The constant levels observed after 500  $^\circ\text{C}$  in TGA curves should correspond to the oxidation of nanotubes. The final residue was analyzed as CdO which revealed thermal stability from 800 to 1000  $^\circ\text{C}$ .

### MWCNTs-COOH/CdO characterization

The possible interaction between  $\text{Cd}(\text{NO}_3)_2$ , MWCNTs-COOH and *N. alba* extract was investigated using FT-IR spectroscopy, which leads the preparation and stabilization of MWCNTs-COOH/CdO. As shown in Figure 4, typical FT-IR spectra of MWCNTs, MWCNTs-COOH and MWCNTs-COOH/CdO can be clarify brieflied.

The bands at around 1300–1550  $\text{cm}^{-1}$  are associated with the vibration of the carbon skeleton of the CNTs. The bands at about 2000–2450  $\text{cm}^{-1}$  are corresponding to the  $\text{C}=\text{C}$  double bonds stretch vibration from the surface of tubes.<sup>[34]</sup> The protein and some chemical compounds from plant extracts might play an important role in the stabilization nanocomposite by binding or encapsulate them. This action forms a layer around nanocomposite and protects them from agglomeration.<sup>[35,36]</sup> In Figure 3(b,c), the bands at about 1630–1750 and 1000–1300  $\text{cm}^{-1}$  indicate the existence of carboxylic groups on the surface of the tube.<sup>[37]</sup> The weak peaks around 3500–3900  $\text{cm}^{-1}$  in Figure 3(b,c) can be assigned to the stretching vibrations of OH groups.<sup>[38,39]</sup> The peaks observed at about 500–700  $\text{cm}^{-1}$  in Figure 3(c) is assigned to the formation of CdO.<sup>[40]</sup> The Ft-IR spectra reveal the different surface chemistry of MWCNTs, MWCNTs-COOH, and MWNTs-COOH/CdO. The peak at about 2300  $\text{cm}^{-1}$  became narrower and the bands around 1630–1750 and 1000–1300  $\text{cm}^{-1}$  are lower in Figure 3(c) than those of pure MWCNTs-COOH Figure 3(b). The result suggested that the surface of MWCNTs-COOH has been covered almost of surface active sites by CdO.

XRD can be used to characterize the crystallization and average size of MWCNT-COOH/CdO. The XRD pattern of MWCNTs-COOH/CdO shows ten intense peaks in the whole spectrum of  $2\theta$  values ranging from  $5^\circ$  to  $80^\circ$ .

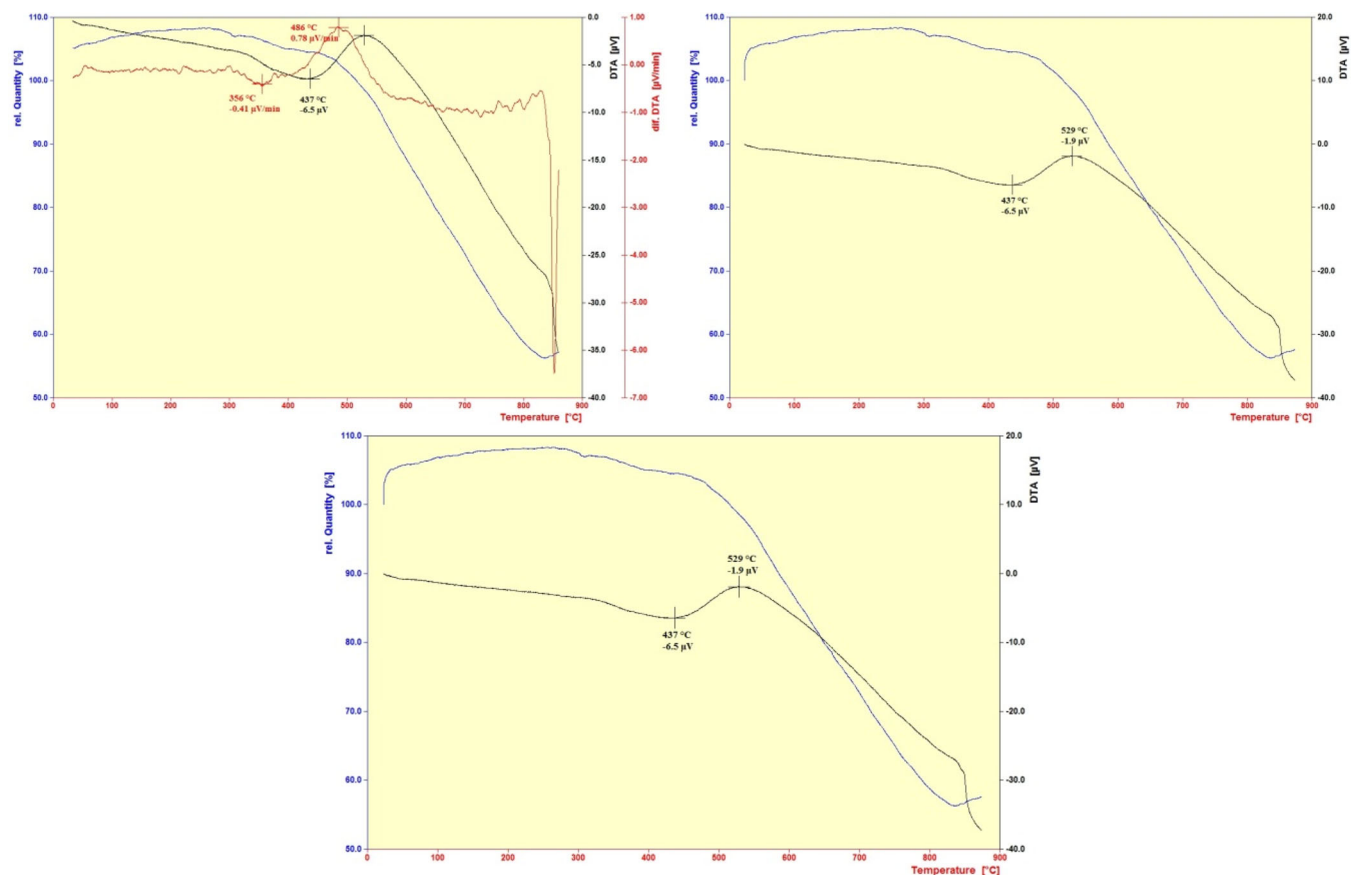


Figure 3. TGA and DTA curves of (MWCNTs)-COOH/CdO nanocomposite.

Presence of six distinct high diffraction peaks at  $2\theta$  values of  $26.598^\circ$ ,  $33.0530^\circ$ ,  $38.351720^\circ$ ,  $55.310^\circ$ ,  $65.931^\circ$  and  $69.268^\circ$ , respectively (JCPDS Number. C: 00-026-1080, and JCPDS Number. CdO: 01-075-0591)<sup>[41–43]</sup> confirmed that the MWCNTs-COOH/CdO had been formed using Water Lily flower extract (Figure 5). The other diffraction peaks could be due to some bioorganic chemical compounds and crystals on the surface of the nanoparticle. The broad X-ray diffraction peaks around their bases indicate that the MWCNTs-COOH/CdO is in nano sizes. With the XRD pattern, the average diameter which can be evaluated from Scherrer equation<sup>[17,44]</sup> ( $D = K\lambda/\beta\cos\theta$ , where  $K$  is constant,  $\lambda$  is X-ray wavelength and  $\beta$  is the peak width at half maximum) is obtained about 76.7 nm.

The morphology and size of MWCNTs-COOH/CdO were studied using transmission electron microscopy (TEM) in Figure 6. It shows the TEM images of MWCNTs-COOH/CdO nanopowders. The TEM image clearly indicates that nanoparticle shape of CdO particle is incorporated on multi wall CNTs and this result is in a good agreement with the result obtained from XRD.

Figure 7 shows the typical SEM images of MWCNTs-COOH/CdO. It is shown that CdO nanoparticles have grown as nanoparticles on the surface of the MWCNTs-COOH.

In Figure 8, energy-dispersive X-ray spectroscopy (EDX) analysis was performed in order to confirm the elements which presented in the resulted MWCNTs-COOH/CdO,

and the analysis reveals the presence of Cd, O and C which emphasize the successful of decoration process with CdO nanoparticles (Scheme 1).

MWCNTs-COOH/CdO was used as a highly efficient catalyst for the synthesis of some heterocyclic compounds. Some pyrimidine derivatives were synthesized by the reaction of thiourea, pyridine or pyrazole derivatives and  $I_2$  in the presence of MWCNTs-COOH/CdO (5% mol) in warm water solution. The assigned structure was further established by CHN analyses, NMR and FT-IR spectra. Because of excellent capacity, the exceedingly simple workup and good yield, eco-friendly catalyst MWCNTs-COOH/CdO were proved to be a good catalyst for this reaction.

In the preliminary stage of the investigation, the model reaction of thiourea, 6-methyl-2-oxo-1,2-dihydro-pyridine-3-carbonitrile, and  $I_2$  was carried out by using various amounts of NPs in various solvents and solvent-free conditions. The optimum amount of MWCNTs-COOH/CdO was 5 mol% as shown in Table 2. Increasing the amount of catalyst does not improve the yield of the product any further, whereas decreasing the amount of catalyst leads to a decrease in the product.

It was found that in the absence of MWCNTs-COOH/CdO, the yield of the product on the TLC plate even after 2h of the reaction wasn't good. The best results were obtained with 5 mol% of MWCNTs-COOH/CdO in warm water under mild reaction conditions (Table 1, entry 4). To evaluate the scope and limitations of this methodology, we

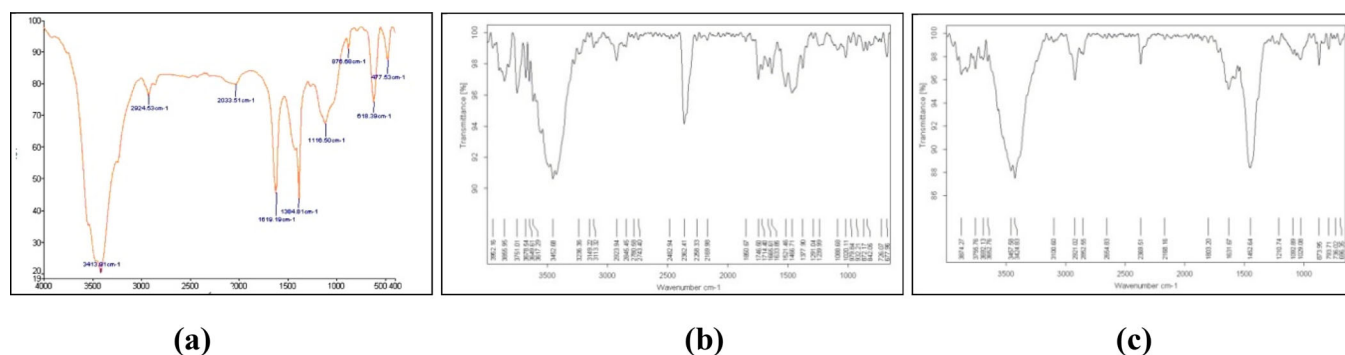


Figure 4. FT-IR spectrum of (a) MWCNTs, (b) biosynthesized MWCNTs-COOH, (d) biosynthesized MWCNTs-COOH/CdO.

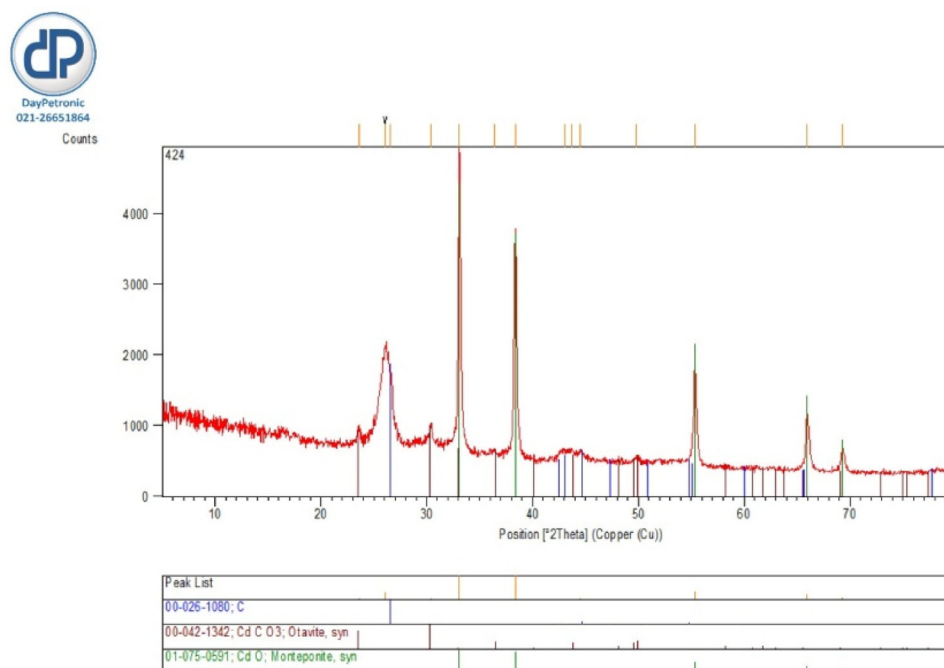


Figure 5. XRD of MWCNTs-COOH/CdO synthesized with Water lily flower extract.

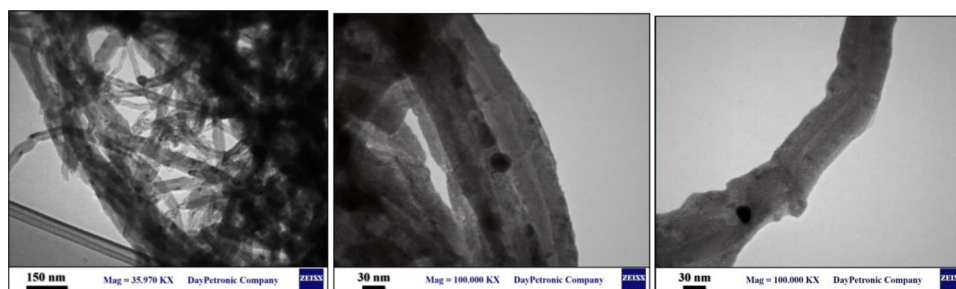


Figure 6. TEM image of MWCNTs-COOH/CdO synthesized with Water lily flower extract.

extended our studies to include a variety of structurally different pyridine or pyrazole derivatives with thiourea. The results are summarized in Table 3 (entries 1–9). In almost all cases, the reactions proceeded smoothly within 60–90 min, providing the corresponding products in good isolated yields.

A plausible mechanism for the reaction is envisaged in (Scheme 2). It is proposed that the carbonyl group and  $I_2$

primarily are activated by MWCNTs-COOH/CdO, and afforded intermediate. At least  $NH_2$  groups of thiourea attack at the C-2 position and CN group of intermediate to obtain 4-Amino-1*H*-pyrido[2,3-*d*]pyrimidine-2-thione derivatives.

The catalyst was simply recovered by centrifugation, washed with ethanol, and dried at 100 °C for 2 h. The recovered catalyst was then added to a fresh reaction mixture

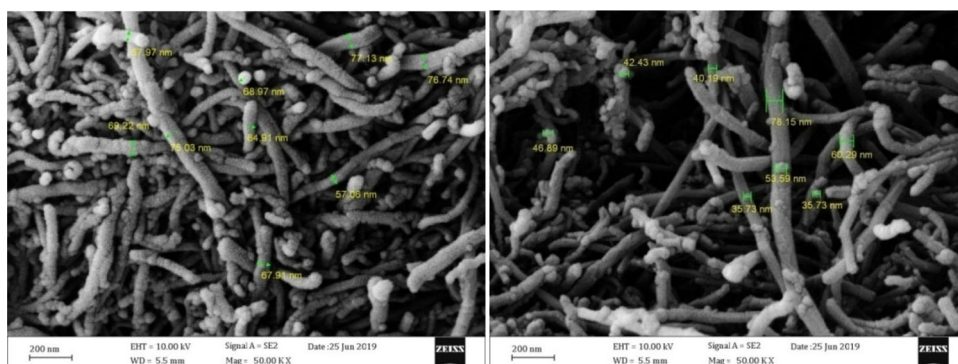


Figure 7. SEM micrograph of MWCNTs-COOH/CdO synthesized with Water lily flower extract.

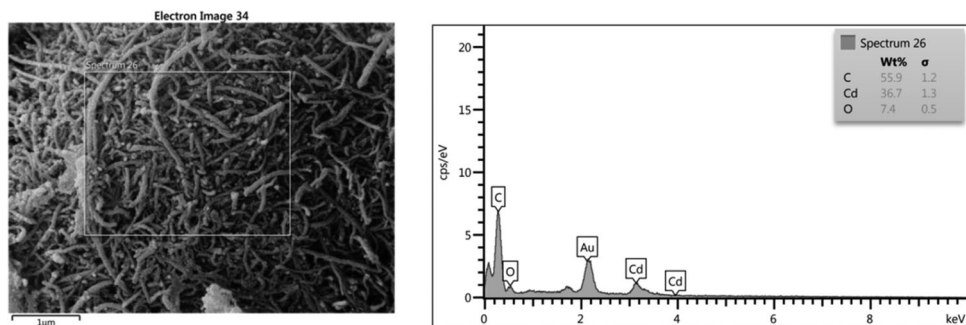
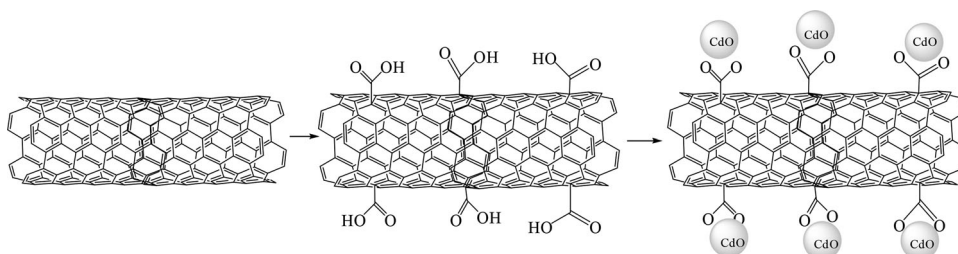


Figure 8. EDX of MWCNTs-COOH/CdO.



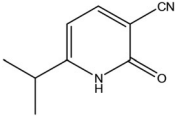
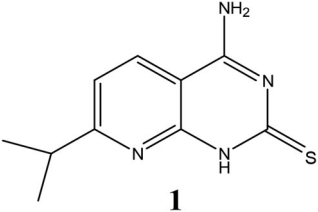
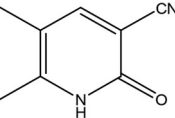
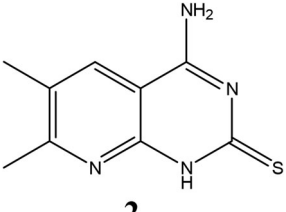
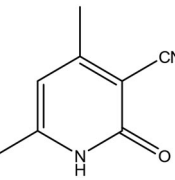
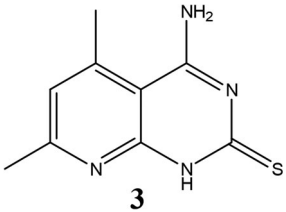
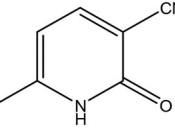
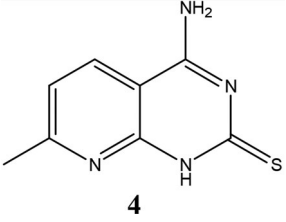
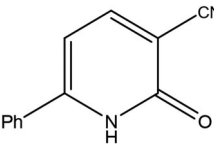
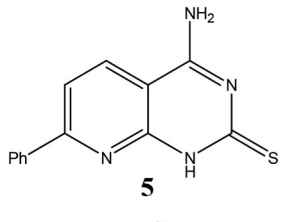
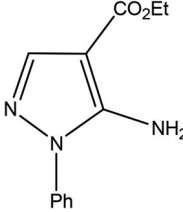
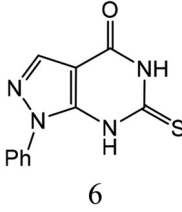
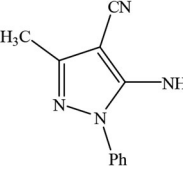
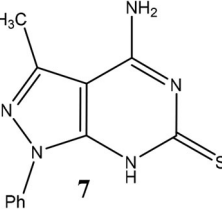
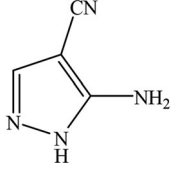
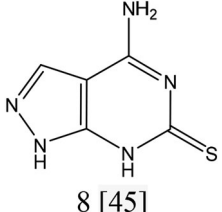
Scheme 1. Preparation of MWCNTs-COOH/CdO nanocomposite with Water lily flower extract

Table 2. Reaction of thiourea (1.2 mmol) with 6-methyl-2-oxo-1,2-dihydro-pyridine-3-carbonitrile (1 mmol) and I<sub>2</sub> (1.2 mmol) under different conditions.

Entry	Solvent	Amount of catalyst MWCNTs-COOH/CdO (mol%)	Time (min)	Yield <sup>a</sup> (%)
1	THF	—	120	Trace
2	THF	3	60	51
3	THF	4	60	58
4	THF	5	60	66
5	THF	7	60	65
6	H <sub>2</sub> O	—	60	Trace
7	H <sub>2</sub> O	3	60	60
8	H <sub>2</sub> O	4	60	85
9	H <sub>2</sub> O	5	40	95
10	H <sub>2</sub> O	7	40	96
11	EtOH	—	120	Trace
12	EtOH	3	60	51
13	EtOH	4	60	64
14	EtOH	5	60	73
15	EtOH	7	60	71
16	CH <sub>2</sub> Cl <sub>2</sub>	—	60	—
17	CH <sub>2</sub> Cl <sub>2</sub>	3	60	33
18	CH <sub>2</sub> Cl <sub>2</sub>	4	60	36
19	CH <sub>2</sub> Cl <sub>2</sub>	5	60	45
19	CH <sub>2</sub> Cl <sub>2</sub>	7	60	46
20	Solvent-free	—	120	40
21	Solvent-free	3	120	50
22	Solvent-free	4	120	68
23	Solvent-free	5	120	74
24	Solvent-free	7	120	76

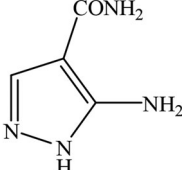
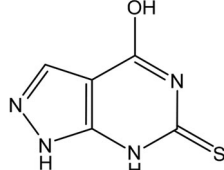
<sup>a</sup>Isolate yield.

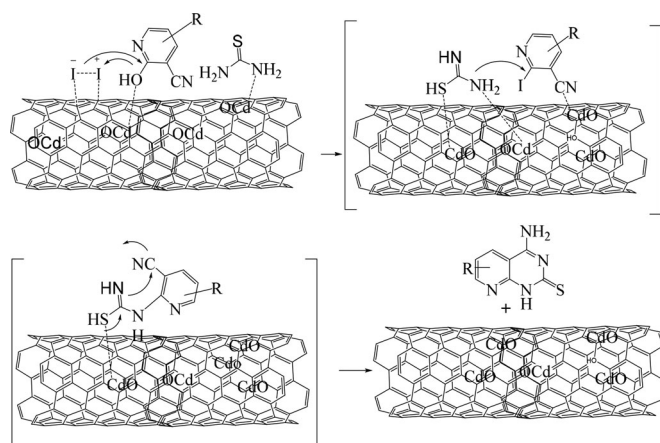
**Table 3.** Production of pyrimidine derivatives using MWCNT-COOH/CdO.

Entry	Amine	Product	Reaction time (min) in H <sub>2</sub> O	m.p.(°C)	Yield%
1		 <b>1</b>	60	>300	85
2		 <b>2</b>	60	148	95
3		 <b>3</b>	60	142	93
4		 <b>4</b>	60	228	96
5		 <b>5</b>	90	174	95
6		 <b>6</b>	90	300	97
7		 <b>7</b>	60	231	93
8		 <b>8 [45]</b>	60	>300	95

(continued)

Table 3. Continued.

Entry	Amine	Product	Reaction time (min) in H <sub>2</sub> O	m.p.(°C)	Yield%
9		 9 [46]	60	>300	96



Scheme 2. A plausible mechanism for synthesis of 4-Amino-1H-pyrido[2,3-d]pyrimidine-2-thione derivatives using MWCNTs-COOH/CdO

Table 4. Recycling of the MWCNT-COOH/CdO catalyst.

No. of cycles	Yield <sup>a</sup> (%)
1	95
2	93
3	89
4	88

<sup>a</sup>Isolate Yield.

under the same conditions and reused 4 times without significant loss of activity (Table 4). Further recycling of the nanocatalyst led to a gradual loss of the catalyst during the recovering and washing stages.

## Conclusions

In this study, we describe biosynthesis of MWCNT-COOH/CdO hybrid by water Lily flower extract and synthesized nanocomposite characterized with UV-Vis spectroscopy, FT-IR, XRD, SEM, EDX and TEM analyses. The results showed Water lily flower extract to be an excellent agent for the synthesis of MWCNT-COOH/CdO hybrid in comparison to some other plant extract. This plant may have the potential for the production of different nanocomposit under mild reaction conditions. In continuation, MWCNT-COOH/CdO was used as an efficient catalyst for the synthesis of some pyrimidine derivatives in a warm water solution. The reactions were carried out in mild reaction conditions and the corresponding products were obtained in good yields. In addition to having the general advantages attributed to the

inherent property of nanocatalyst, MWCNT-COOH/CdO hybrid exhibited exceptionally high catalytic activity in heterocyclic chemistry and increases reaction speed without pollution. This method is easier and less expensive than other methods.

## Acknowledgment

The authors wish to thanks Islamic Azad University in Qaemshahr Branch for the institutional support.

## Disclosure statement

No potential conflict of interest was reported by the authors.

## References

- Alshehri, R.; Ilyas, A. M.; Hasan, A.; Arnaout, A.; Ahmed, F.; Memic, A. Carbon Nanotubes in Biomedical Applications: Factors, Mechanisms, and Remedies of Toxicity. *J. Med. Chem.* **2016**, *59*, 8149–8167. DOI: [10.1021/acs.jmedchem.5b01770](https://doi.org/10.1021/acs.jmedchem.5b01770).
- Vashist, S. K.; Zheng, D.; Pastorin, G.; Al-Rubeaan, K.; Luong, J. H. T.; Sheu, F. S. Delivery of Drugs and Biomolecules Using Carbon Nanotubes. *Carbon* **2011**, *49*, 4077–4097. DOI: [10.1016/j.carbon.2011.05.049](https://doi.org/10.1016/j.carbon.2011.05.049).
- Tan, C. M.; Baudot, C.; Han, Y.; Jing, H. Applications of Multi-Walled Carbon Nanotube in Electronic Packaging. *Nanoscale Res. Lett.* **2012**, *7*, 183–189. DOI: [10.1186/1556-276X-7-183](https://doi.org/10.1186/1556-276X-7-183).
- Cheng, Y.; Xu, C.; Jia, L.; Gale, J. D.; Zhang, L.; Liu, C.; Shen, P. K.; Jiang, S. P. Pristine Carbon Nanotubes as Non-Metal Electrocatalysts for Oxygen Evolution Reaction of Water Splitting. *Appl. Catal. B.* **2015**, *163*, 96–104. DOI: [10.1016/j.apcatb.2014.07.049](https://doi.org/10.1016/j.apcatb.2014.07.049).
- Ghodselahi, T.; Soleymani, S.; Akbarzadeh Pasha, M.; Vesaghi, M. A. Ni Nanoparticle Catalyzed Growth of MWCNTs on Cu NPs@ a-C: H Substrate. *Eur. Phys. J. D.* **2012**, *66*, 299–303. DOI: [10.1007/s40089-016-0197-4](https://doi.org/10.1007/s40089-016-0197-4).
- Chen, C. S.; Liu, T. G.; Lin, L. W.; Xie, X. D.; Chen, X. H.; Liu, Q. C.; Liang, B.; Yu, W. W.; Qiu, C. Y. Multi-Walled Carbon Nanotube-Supported Metal-Doped ZnO Nanoparticles and Their Photocatalytic Property. *J. Nanopart. Res.* **2013**, *15*, 1295–1304. DOI: [10.1007/s11051-012-1295-5](https://doi.org/10.1007/s11051-012-1295-5).
- Lu, Y.; Yu, G.; Wei, X.; Zhan, C.; Jeon, J.-W.; Wang, X.; Jeffryes, C.; Guo, Z.; Wei, S.; Wujcik, E. K. Fabric/Multi-Walled Carbon Nanotube Sensor for Portable on-Site Copper Detection in Water. *Adv. Compos. Hybrid Mater.* **2019**, *2*, 711–719. DOI: [10.1007/s42114-019-00122-7](https://doi.org/10.1007/s42114-019-00122-7).
- Roldo, M.; Fatouros, D. G.; Hallaj, R.; Deng, L.; Zhu, C.; Dong, S.; Zhuo, Y.; Strano, M. S.; Hara, K.; Haniu, H.; et al. Biomedical Applications of Carbon Nanotubes. *Annu. Rep. Prog. Chem., Sect. C: Phys. Chem.* **2013**, *109*, 10. DOI: [10.1039/c3pc90010j](https://doi.org/10.1039/c3pc90010j).
- Mehrabi, M.; Parvin, P.; Reyhani, A.; Mortazavi, S. Z. Hydrogen Storage in Multi-Walled Carbon Nanotubes Decorated with

- Palladium Nanoparticles Using Laser Ablation/Chemical Reduction Methods. *Mater. Res. Express* **2017**, *4*, 095030. DOI: [10.1088/2053-1591/aa87f6](https://doi.org/10.1088/2053-1591/aa87f6).
10. Keru, G.; Ndungu, P. G.; Nyamori, V. O. A Review on Carbon Nanotube/Polymer Composites for Organic Solar Cells. *Int. J. Energy Res.* **2014**, *38*, 1635–1653. DOI: [10.1002/er.3194](https://doi.org/10.1002/er.3194).
  11. Dalouji, V.; Elahi, S. M.; Solaymani, S.; Ghaderi, A. Absorption Edge and the Refractive Index Dispersion of Carbon-Nickel Composite Films at Different Annealing Temperatures. *Eur. Phys. J. Plus* **2016**, *131*, 84–90. DOI: [10.1140/epjp/i2016-16084-8](https://doi.org/10.1140/epjp/i2016-16084-8).
  12. Bai, W.; Wu, Z.; Mitra, S.; Brown, J. M. Effects of Multiwalled Carbon Nanotube Surface Modification and Purification on Bovine Serum Albumin Binding and Biological Responses. *J. Nanomater.* **2016**, *2016*, 1–10. DOI: [10.1155/2016/2159537](https://doi.org/10.1155/2016/2159537).
  13. V, L. K.; Ntim, S. A.; Sae-Khow, O.; Janardhana, C.; Lakshminarayanan, V.; Mitra, S. Electro-Catalytic Activity of Multiwall Carbon Nanotube-Metal (Pt or Pd) Nanohybrid Materials Synthesized Using Microwave-Induced Reactions and Their Possible Use in Fuel Cells. *Electrochim. Acta.* **2012**, *83*, 40–46. DOI: [10.1016/j.electacta.2012.07.098](https://doi.org/10.1016/j.electacta.2012.07.098). [[23118490](https://doi.org/10.1016/j.electacta.2012.07.098)]
  14. Hai, T. L.; Hung, L. C.; Phuong, T. T. B.; Ha, B. T. T.; Nguyen, B.-S.; Hai, T. D.; Nguyen, V.-H. Multiwall Carbon Nanotube Modified by Antimony Oxide (Sb<sub>2</sub>O<sub>3</sub>/MWCNTs) Paste Electrode for the Simultaneous Electrochemical Detection of Cadmium and Lead Ions. *Microchem. J.* **2020**, *153*, 104456. DOI: [10.1016/j.microc.2019.104456](https://doi.org/10.1016/j.microc.2019.104456).
  15. Eder, D. Carbon Nanotube-Inorganic Hybrids. *Chem. Rev.* **2010**, *110*, 1348–1385. DOI: [10.1021/cr800433k](https://doi.org/10.1021/cr800433k).
  16. Kumari, C. *Nanomaterials for the Life Sciences*; Wiley: Hoboken, **2010**, Chapt. 16, pp. 403–418.
  17. Rahmanifar, E.; Yoosefian, M.; Karimi-Maleh, H. Application of CdO/SWCNTs Nanocomposite Ionic Liquids Carbon Paste Electrode as a Voltammetric Sensor for Determination of Benserazide. *CAC* **2016**, *13*, 46–51. DOI: [10.2174/1573411012666160601145809](https://doi.org/10.2174/1573411012666160601145809).
  18. Singh, G.; Kapoor, I. P. S.; Dubey, R.; Srivastava, P. Synthesis, Characterization and Catalytic Activity of CdO Nanocrystals. *Mater. Sci. Eng., B.* **2011**, *176*, 121–126. DOI: [10.1016/j.mseb.2010.10.009](https://doi.org/10.1016/j.mseb.2010.10.009).
  19. Bulakhe, R. N.; Lokhande, C. D. Chemically Deposited Cubic Structured CdO Thin Films: Use in Liquefied Petroleum Gas Sensor. *Sens. Actuators, B.* **2014**, *200*, 245–250. DOI: [10.1016/j.snb.2014.04.061](https://doi.org/10.1016/j.snb.2014.04.061).
  20. Gulino, G.; Compagnini, A.; Scalisi, A. Large Third-Order Nonlinear Optical Properties of Cadmium Oxide Thin Films. *Chem. Mater.* **2003**, *15*, 3332–3336. DOI: [10.1021/cm031075f](https://doi.org/10.1021/cm031075f).
  21. Mane, R. S.; Pathan, H. M.; Lokhande, C. D.; Han, S.-H. An Effective Use of Nanocrystalline CdO Thin Films in Dye-Sensitized Solar Cells. *Sol. Energy* **2006**, *80*, 185–190. DOI: [10.1016/j.solener.2005.08.013](https://doi.org/10.1016/j.solener.2005.08.013).
  22. Salehi, B.; Mehrabian, S.; Ahmadi, M. Investigation of Antibacterial Effect of Cadmium Oxide Nanoparticles on Staphylococcus aureus Bacteria. *J. Nanobiotechnol.* **2014**, *12*, 26–34. DOI: [10.1186/s12951-014-0026-8](https://doi.org/10.1186/s12951-014-0026-8).
  23. Savale, A.; Ghotekar, S.; Pansambal, S. Green Synthesis of Fluorescent CdO Nanoparticles Using Leucaena Leucocephala L. Extract and Their Biological Activities. *J. Bacteriol. Mycol.* **2017**, *5*, 373–376. DOI: [10.15406/jbmoa.2017.05.00148](https://doi.org/10.15406/jbmoa.2017.05.00148).
  24. Ghotekar, S. A Review on Plant Extract Mediated Biogenic Synthesis of CdO Nanoparticles and Their Recent Applications. *Asian J. Green Chem.* **2019**, *3*, 187–200. DOI: [10.22034/ajgc.2018.140313.1084](https://doi.org/10.22034/ajgc.2018.140313.1084).
  25. Afolayan, A. J.; Sharaibi, O. J.; Kazeem, M. I. Phytochemical Analysis and in Vitro Antioxidant Activity of Nymphaea lotus L. *Int. J. Pharmacol.* **2013**, *9*, 297–304. DOI: [10.3923/ijp.2013.297.304](https://doi.org/10.3923/ijp.2013.297.304).
  26. Bakr, O.; El-Naa, M. M.; Zaghoul, S. S.; Omar, M. M. Profile of Bioactive Compounds in *Nymphaea alba* L. Leaves Growing in Egypt: Hepatoprotective, Antioxidant and anti-inflammatory activity. *BMC Complem. Altern Med.* **2017**, *17*, 52–64. DOI: [10.1186/s12906-017-1561-2](https://doi.org/10.1186/s12906-017-1561-2).
  27. Bakr, R. O.; Wasfi, R.; Swilam, N.; Sallam, I. E. Characterization of the Bioactive Constituents of Nymphaea alba Rhizomes and Evaluation of anti-Biofilm as Well as Antioxidant and Cytotoxic Properties. *J. Med. Plants Res.* **2016**, *10*, 390–401. DOI: [10.5897/JMPR2016.6162](https://doi.org/10.5897/JMPR2016.6162).
  28. Asadi, Z.; Nami, N.; Hosseinzadeh, M. Green Synthesis and Characterization of Silver Nanoparticles (Ag NPs) Using White Water Lily Flower Extraction Species Nymphaea alba of Nymphaeaceae Family. *Iran. J. Organ. Chem.* **2018**, *10*, 2403–2408.
  29. Khan, W.; Sharma, R.; Chaudhury, P. K.; Siddiqui, A. M.; Saini, P. Synthesis of Carboxylic Functionalized Multi Wall Carbon Nanotubes and Their Application for Static Charge Dissipative Fibers. *Int. J. Nanomater. Nanotechnol. Nanomed.* **2016**, *2*, 025–028. DOI: [10.17352/2455-3492.000011](https://doi.org/10.17352/2455-3492.000011).
  30. Zahera, M.; Khan, S. A.; Khan, I. A.; Sharma, R. K.; Sinha, N.; Al-Shwaiman, H. A.; Al-Zahrani, R. R.; Elgorban, A. M.; Syed, A.; Khan, M. S. Cadmium Oxide Nanoparticles: An Attractive Candidate for Novel Therapeutic Approaches. *Colloids Surf. A.* **2020**, *585*, 124017. DOI: [10.1016/j.colsurfa.2019.124017](https://doi.org/10.1016/j.colsurfa.2019.124017).
  31. Jiang, L.; Gao, L.; Sun, J. Production of Aqueous Colloidal Dispersions of Carbon Nanotubes. *J. Colloid Interf. Sci.* **2003**, *260*, 89–94. DOI: [10.1016/S0021-9797\(02\)00176-5](https://doi.org/10.1016/S0021-9797(02)00176-5).
  32. Daraio, X. R.; Ye, C.; Wang, C.; Talbot, J. B.; Jin, S. Room Temperature Solvent-Free Synthesis of Monodisperse Magnetite Nanocrystals. *J. Nanosci. Nanotechnol.* **2006**, *6*, 852–856. DOI: [10.1166/jnn.2006.135](https://doi.org/10.1166/jnn.2006.135).
  33. Guo-Hua, Z.; Ming-Fang, L.; Ming-Li, L. Differential Pulse Voltammetric Determination of Dopamine with the Coexistence of Ascorbic Acid on Boron-Doped Diamond Surface. *CEJC* **2007**, *5*, 1114–1123. DOI: [10.2478/s11532-007-0049-1](https://doi.org/10.2478/s11532-007-0049-1).
  34. Hwa, K.-Y.; Subramani, B. Synthesis of Zinc Oxide Nanoparticles on Graphene-Carbon Nanotube Hybrid for Glucose Biosensor Applications. *Bioelectron.* **2014**, *62*, 127–133. DOI: [10.1016/j.bios.2014.06.023](https://doi.org/10.1016/j.bios.2014.06.023).
  35. Chandran, S. P.; Chaudhary, M.; Pasricha, R.; Ahmad, A. M.; Sastry, M. Synthesis of Gold Nanotriangles and Silver Nanoparticles Using Aloe Vera Plant Extract. *Biotechnol. Prog.* **2006**, *22*, 577–583. DOI: [10.1021/bp0501423](https://doi.org/10.1021/bp0501423).
  36. Pontaza-Licon, Y. S.; Ramos-Jacques, A. L.; Cervantes-Chavez, J. A.; LuisLópez-Miranda, J.; Ruiz-Baltazar, Á. J.; Maya-Cornejo, J.; Rodriguez-Morales, A. L.; Esparza, R.; Estevez, M.; Pérez, R.; Hernandez-Martínez, A. R. Alcoholic Extracts from Paulownia tomentosa Leaves for Silver Nanoparticles Synthesis. *Results Phys.* **2019**, *12*, 1670–1679. DOI: [10.1016/j.rinp.2019.01.082](https://doi.org/10.1016/j.rinp.2019.01.082).
  37. Hamadani, M.; Jabbari, V.; Shamshiri, M.; Asad, M.; Mutlay, I. Preparation of Novel Hetero-Nanostructures and High Efficient Visible light-Active Photocatalyst Using Incorporation of CNT as an Electron-Transfer Channel into the Support TiO<sub>2</sub> and PbS. *J. Taiwan Inst. Chem. Eng.* **2013**, *44*, 748–757. DOI: [10.1016/j.jtice.2013.01.018](https://doi.org/10.1016/j.jtice.2013.01.018).
  38. Balamurugan, S.; Balu, A. R.; Usharani, K.; Suganya, M.; Anitha, S.; Prabha, D.; Ilango, S. Synthesis of CdO Nanopowders by a Simple Soft Chemical Method and Evaluation of Their Antimicrobial Activities. *Pac. Sci. Rev. A: Nat. Sci. Eng.* **2016**, *18*, 228–232. DOI: [10.1016/j.psra.2016.10.003](https://doi.org/10.1016/j.psra.2016.10.003).
  39. Atieh, M. A.; Bakather, O. Y.; Al-Tawbini, B.; Bukhari, A. A.; Abulilwi, F. A.; Fettouhi, M. B. Effect of Carboxylic Functional Group Functionalized on Carbon Nanotubes Surface on the Removal of Lead from Water. *Bioinorg. Chem. Appl.* **2010**, *2010*, 1–9. DOI: [10.1155/2010/603978](https://doi.org/10.1155/2010/603978).
  40. Anandhan, K.; Thilak Kumar, R. Synthesis, FTIR, UV-Vis and Photoluminescence Characterizations of Triethanolamine Passivated CdO Nanostructures. *Spectrochim. Acta A. Mol. Biomol. Spectrosc.* **2015**, *149*, 476–480. DOI: [10.1016/j.saa.2015.04.035](https://doi.org/10.1016/j.saa.2015.04.035).
  41. Alaf, M.; Gultekin, D.; Akbulut, H. Production of Sn/SnO<sub>2</sub>/MWCNT Composites by Plasma Oxidation after Thermal Evaporation from Pure Sn Targets onto Buckypapers. *J. Nanosci. Nanotechnol.* **2012**, *12*, 9058–9066. DOI: [10.1166/jnn.2012.6753](https://doi.org/10.1166/jnn.2012.6753).

42. Borodin, V. L.; Lyutin, V. I.; Ilyukhin, V. V.; Belov, N. V. Calcite-Otavite Isomorphous Series. *Dokl. Akad. Nauk SSSR* **1979**, *245*, 1099–1101.
43. Mwafy, E., Mostafa, A. M. Multi Walled carbon nanotube decorated cadmium oxide nanoparticles via pulsed laser ablation liquid media. *Optics & Laser Technology*. **2019**, *111*, 249–254. DOI: [10.1016/j.optlastec.2018.09.055](https://doi.org/10.1016/j.optlastec.2018.09.055).
44. Warren, B. E. *X-Ray Diffraction*. Courier Corporation: North Chelmsford, **1990**.
45. Tominaga, Y.; Honkawa, Y.; Hara, M.; Hosomi, A. Synthesis of Pyrazolo[3,4-d]Pyrimidine Derivatives Using Ketene Dithioacetals. *J. Heterocycl.Chem.* **1990**, *27*, 775–783. DOI: [10.1002/jhet.5570270355](https://doi.org/10.1002/jhet.5570270355).
46. Kim, D. C.; Lee, Y. R.; Yang, B. S.; Shin, K. J.; Kim, D. J.; Chung, B. Y.; Yoo, K. H. Synthesis and Biological Evaluations of Pyrazolo[3,4-d]Pyrimidines as Cyclin-Dependent Kinase 2 Inhibitors. *Eur. J. Med. Chem* **2003**, *38*, 525–532. DOI: [10.1016/S0223-5234\(03\)00065-5](https://doi.org/10.1016/S0223-5234(03)00065-5).